Published in final edited form as:
Tetrahedron. 2014 July 8; 70(27-28): 4245–4249. doi:10.1016/j.tet.2014.03.008.

Manganese terpyridine artificial metalloenzymes for benzylic oxygenation and olefin epoxidation

Chen Zhang, **Poonam Srivastava**, **Ken Ellis-Guardiola**, and **Jared C. Lewis**[*,a]

[a]Department of Chemistry, University of Chicago, 5735 S. Ellis Ave., Chicago, IL 60637 (USA)

Abstract

New catalysts for non-directed hydrocarbon functionalization have great potential in organic synthesis. We hypothesized that incorporating a Mn-terpyridine cofactor into a protein scaffold would lead to artificial metalloenzymes (ArMs) in which the selectivity of the Mn cofactor could be controlled by the protein scaffold. We designed and synthesized a maleimide-substituted Mn-terpyridine cofactor and demonstrated that this cofactor could be incorporated into two different scaffold proteins to generate the desired ArMs. The structure and reactivity of one of these ArMs was explored, and the broad oxygenation capability of the Mn-terpyridine catalyst was maintained, providing a robust platform for optimization of ArMs for selective hydrocarbon functionalization.

Keywords

Artificial metalloenzyme; Manganese; C-H functionalization; Epoxidation; Biocatalysis

1. Introduction

New catalysts for non-directed hydrocarbon functionalization have great potential for applications in organic synthesis.[1,2] By avoiding the need for directing groups, these species expand the range of substrates on which they can act and eliminate synthetic steps and byproducts associated with directing group installation and removal.[3] A number of catalysts, including dirhodium tetracarboxylate complexes[4] and several different iron[5] and manganese[6,7] complexes, are particularly notable in this regard and are widely used for insertion of carbene,[8] nitrene,[8] and oxo[9] fragments into C-H bonds and olefins. While reactivity trends for such catalysts have been outlined, controlling their selectivity,[9] particularly on complex substrates,[1,2] remains difficult.

[*]Corresponding author: Tel.: +1-773-702-3456; fax: +1-773-702-0805; jaredlewis@uchicago.edu.

Supplementary Material

Supplementary materials, including ESI-MS, HPLC, and NMR characterization of synthetic intermediates and more experimental details associated with this article, can be found online.

Crabtree and Brudvig have demonstrated that the selectivity of Kemp's-triacid-based Mn-terpyridine complexes for oxygenation of certain carboxylic acid-substituted substrates can be controlled by catalyst-substrate hydrogen bonding.[10–13] The reported examples illustrate the potential for supramolecular interactions to control the selectivity of Mn-terpyridine catalysts but require the use of a carboxylic acid directing group. We hypothesized that incorporating Mn-terpyridine cofactors into protein scaffolds would lead to artificial metalloenzymes (ArMs)[14] in which the selectivity of the Mn cofactor could be controlled by substrate binding to the protein. Mn-terpyridine complexes catalyze a number of oxygenation reactions,[15] ethereal α-C-H oxidation,[15] and hydrocarbon desaturation,[16] suggesting that the proposed ArMs could possess broad reaction scope. The utility of ArMs for selective catalysis has been demonstrated for a number of different reactions.[17] Hayashi recently demonstrated that myoglobin reconstituted with a Mn-porphycene cofactor catalyzes benzylic oxygenation,[18] but we are unaware of any reports of similar reactions using ArMs generated via covalent scaffold modification[14]. While biocatalysts (e.g. cytochromes P450) for this reaction exist, altering their substrate scope and site selectivity can be challenging.[19,20] The potential ease with which a Mn-terpyridine cofactor could be incorporated into different proteins[21] to modulate selectivity led us to develop a robust platform to explore the feasibility of this approach.

2. Result and discussion

Maleimide-substituted cofactor **3** was synthesized[22,23] from the known amine-substituted terpyridine, **1**[24,25] (Scheme 1).

Cysteine mutants of tHisF[26] and aponitrobindin (Nb)[27] were then prepared as scaffolds for initial bioconjugation studies. Both of these proteins have been used as ArM scaffolds by us[28] and by others[29,30] and therefore serve as ideal substrates for initial studies on cofactor bioconjugation using **3**. Reacting tHisF-C48 with **3** provided modest conversion (ca. 40%) to tHisF-C48-**3** within 2h (Table 1, entry 1), but longer reaction times appeared to give multiple addition products (ESI-MS, data not shown), a common problem with maleimide bioconjugation reactions[31]. On the other hand, we found that mutating a leucine residue (L50) located directly above C48 in the β-barrel of tHisF[26] led to a marked increase in bioconjugation rate and selectivity, and over 80% conversion to tHisF-C48A50-**3** was achieved within 2h (entry 2). These improvements presumably resulted from decreased steric hindrance proximal to the cysteine nucleophile.

Nitrobindin is a heme protein with a β-barrel structure and a large hydrophobic pocket for heme binding. Cysteine mutations at suitable locations within the β-barrel can be used to position cofactors within the heme binding pocket of the apo enzyme (Nb).[30] Bioconjugation of two cysteine mutants of Nb, C96 within the β-barrel and C125 on the protein surface, were examined, and both of these provided greater than 90% conversion to the corresponding Nb-C-**3** bioconjugates (entries 3 and 4). These results, in addition to those noted above using tHisF, highlight two key advantages of covalent bioconjugation for ArM formation:[21] the nature of both the scaffold itself and the local environment of the bioconjugation site can be readily manipulated to facilitate cofactor installation[14].

Following characterization of Nb-C96-**3**, the reactivity of this ArM under a variety of conditions was explored to examine the impact of confining the Mn center within the heme binding pocket. Benzylic oxygenation of ibuprofen methyl ester (**4a**) was initially investigated based on previous reports from Crabtree and Brudvig.[13] As previously noted, these researchers reported that ibuprofen (**5a**) oxygenation can be catalyzed by Kemp's-triacid-based Mn-terpyridine complexes to provide a mixture of **5b** and **5c**, the latter resulting from decarboxylation following oxygenation (Table 3). The selectivity of this reaction could be controlled using hydrogen bonding between carboxylic acid groups on ibuprofen and the catalyst, with the presence of the carboxylic acid on the catalyst improving the **5b:5c** ratio from 77:23 to 98.5:1.5.

We found that similar benzylic oxygenation and oxygenation/decarboxylation of **4a** was catalyzed by Nb-C96-**3** (Table 2). Oxone, peracids, and a number of additional oxidants are known to promote Mn-terpyridine catalyzed oxygenation, and both oxone and peroxyacetic acid proved to be compatible with Nb-C96-**3**. Crucial to this reactivity, however, was the use of phosphate buffer (Table 2, entries 1–3). A modest excess of peroxyacetic acid was sufficient to achieve maximum conversion, and this helped to minimize pH changes over the course of the reaction (entries 3–5). While the Nb scaffold can tolerate 20% v/v acetonitrile, greater than this amount led to protein precipitation and dramatically reduced conversion. Maximum conversion was observed using 10% v/v acetonitrile, and omitting acetonitrile entirely led to reduced conversion, presumably due to poor substrate solubility (entries 5–8). Conducting the reactions at room temperature or decreasing ArM loading to 2.5 mol% both led to significant decreases in conversion (entries 9–10). All reactions in Table 2 provided a similar **4b:4c** ratio of 88:12. Nb-C125-**3** provided this same ratio with slightly higher conversion, suggesting that improved substrate access to **3** attached to the protein surface (in Nb-C125-**3**) offset any potential scaffold acceleration[32] afforded by the heme binding pocket (in Nb-C96-**3**).

The optimized conditions identified in Table 2, entry 7 were then used to explore the substrate scope of Nb-C96-**3** catalyzed oxygenation.[15] Both ibuprofen methyl ester and ibuprofen provided high conversions (Table 3, Entry 1), and benzylic oxygenation (**4**/**5b**) and decarboxylation (**4**/**5c**) products were formed in similar ratios. Isochroman (**6a**) underwent benzylic oxygenation with a preference for the more activated 1-position (entry 2), while 9,10-dihydrophenanthrene (**7a**) was oxidized to a mixture of diketone **7b** and phenanthrene (entry 3). Epoxidation of different olefins was also examined. Styrene and the β-substituted styrylacetic acid methyl ester were both epoxidized in good yield (entries 4 and 5). Cyclic cis-internal olefins were particularly reactive substrates, and nearly quantitative epoxidation of both chromene **10a** and norbornene-2-carboxylate methyl ester **11a** was observed (entries 6 and 7). Finally, ethereal α-C-H oxidation of cyclohexyl methyl ether **12a**, which proceeds via C-H hydroxylation followed by hemiacetal decomposition, was also observed in moderate yield (Entry 8).

The substrate scope outlined in Table 3 shows that the broad reactivity of Mn-terpyridine complexes toward hydrocarbon oxidation[15] is not compromised in the context of a protein scaffold. In general, a slight decrease in reaction rate was observed using Nb-C96-**3** relative to **3** (see supporting information), but otherwise similar reactivity was observed. In entries

1–3, product mixtures were obtained, and while no difference between the selectivities of **3** and Nb-C96-**3** was observed, these substrates will serve as valuable probes to explore the impact of scaffold mutations on oxygenation selectivity in future studies.[33,34] A preliminary investigation of epoxidation enantioselectivity revealed that an e.r. of 53.5:46.5 was observed in the reaction of **10a** (racemic product was obtained using **3**; see supporting information), while the remaining olefins provided racemic product. While obviously low, this result provides a starting point for engineering scaffold mutants with improved selectivity.[33,34]

3. Conclusions

Maleimide-substituted manganese terpyridine cofactor **3** was prepared and reacted with cysteine mutants of tHisF and Nb scaffold proteins to generate the desired ArMs in good to excellent yield based on HR ESI-MS. Spectroscopic characterization (CD and UV) of Nb-C96-**3** provided additional details on the structure of this bioconjugate, confirming both the nature of the scaffold fold and the presence of the $MnCl_2$ fragment. Nb-C96-**3** catalyzed hydrocarbon oxygenation in the presence of either Oxone or AcOOH, and optimized reaction conditions enabled benzylic oxygenation, olefin epoxidation, and heteroatom demethylation[15]. The substrates examined, in conjunction with the robust ArM reactivity observed, will enable exploration of the impact of scaffold structure on the regio-, enantio-, and chemo-selectivity of **3**. Toward this end, we are currently examining a range of cofactor linkage sites within the Nb scaffold as well as mutagenesis of residues proximal to the Mn center in Nb-C96-**3**. The generality of the covalent linkage method employed[21] will also enable facile exploration of additional scaffold proteins to identify systems with unique hydrocarbon oxygenation selectivity.

4. Experimental Section

All reagents were obtained from commercial suppliers and used without further purification. Acetonitrile (ACN), tetrahydrofuran (THF) and dichloromethane (DCM) were obtained from a PureSolv MD solvent purification system by Innovative Technology (solvent deoxygenated by N_2 sparge and dried over alumina). “Extra Dry” grade methanol purchased from Acros was used. Deuterated solvents were obtained from Cambridge Isotope Labs. Known compound **1** was prepared as previously reported.

4.1. Cloning, Expression and Purification of Nitrobindin Protein

A codon optimized gene for Nitrobindin protein (Nb, PDB ID 3EMM) was obtained from GenScript (Piscataway, NJ) and cloned into pET22b using NdeI and XhoI restriction sites. A gene encoding the cyclase subunit of the imidazole glycerol phosphate synthase enzyme complex from *Thermotoga maritima* (tHisF, PDB ID 1THF) was amplified from pET11c-tHisF20 by PCR using gene specific primers containing NdeI (forward) and XhoI (reverse) restriction sites. Both the genes were cloned such that they would expresses with a C-terminal hexa-histidine tag for Ni-NTA affinity chromatography. Overlap extension PCR was used to introduce point mutations, and all constructs were confirmed by sequencing. Mutations encoding a Cysteine (TGC) at desired locations (C96 and C125 for Nb and C48 for tHisF) were introduced for ArM formation. For the tHisF double mutant (C48A50),

leucine was replaced by alanine using overlap extension PCR with the gene encoding tHisF-C48 as a template.

For expression, mutants were transformed into *E. coli* BL21 (DE3) cells. The cells were recovered in LB for 1 h at 37 °C and then plated on LB/agar plates containing 100μg/mL ampicillin. Single colonies were picked and used to inoculate 2YT media containing 100μg/mL ampicillin. The resulting cultures were incubated at 37 °C while shaking at 250 RPM until the OD_{600} reached approximately 1.0, at which point IPTG was added to final concentrations of 1mM. After incubating for 16 h post induction, cells were harvested by centrifugation and lysed in phosphate-buffered saline (pH 7.5) by sonication. The crude lysate was clarified by centrifugation at 16000g at 4 °C for 30 min. The clarified lysate was then purified by Ni-NTA affinity chromatography at 4 °C. Pure protein was eluted using 50 mM NaH_2PO_4/300 mM NaCl/250 mM imidazole (pH 8.0) and the purified Nb was concentrated and stored in Tris buffer (10mM pH 7.5) using 10 kDa cutoff spin filters (Millipore).

4.2. Cofactor (3) synthesis

4.2.1. N-[2-([2,2′:6′,2″-terpyridin]-4′-yloxy) ethylmaleimide (2)—To a solution of **1** (292 mg, 1 mmol) in CH_2Cl_2 (10 mL) was added maleic anhydride (490 mg, 5 mmol). The mixture was heated at reflux for 3.5 h and subsequently cooled to room temperature. A white precipitate formed, was collected by filtration, and was washed with cold CH_2Cl_2. The solid was then added to a suspension of NaOAc (1 g) in Ac_2O (10 mL), and the resulting mixture was heated at reflux for 1 h. The mixture was cooled to room temperature, poured into ice-water (40 mL), and stirred for 2 h. The mixture was extracted with CH_2Cl_2 (3×100 mL), and the combined organic extracts were washed sequentially with saturated $NaHCO_3$ (3×50mL), H_2O (1×50 mL), and brine (1×50 mL), and dried over $MgSO_4$. Removing the solvent using rotary evaporation provided the desired product as a white solid; yield: 219 mg (0.589 mmol, 59%). ^{1}H NMR (500 MHz, $CDCl_3$): δ 8.72 (d, J = 4.6 Hz, 2H), 8.64 (d, J = 7.9 Hz, 2H), 8.02 (s, 2H), 7.88 (td, J = 7.7, 1.7 Hz, 2H), 7.37 (dd, J = 6.9, 5.3 Hz, 2H), 6.79 (s, 2H), 4.45 (t, J = 5.6 Hz, 2H), 4.08 (t, J = 5.6 Hz, 2H). ^{13}C NMR (500 MHz, CDCl3): δ 170.5, 166.6, 157.3, 156.0, 149.2, 137.0, 134.4, 124.0, 121.5, 107.4, 64.9, 37.1. HRMS-ESI (m/z): for $C_{21}H_{16}N_4O_3$, calculated: 373.1295, found: 373.1290.

4.2.2. Manganese (II) terpyridine complex (3)—Manganese chloride tetrahydrate (212 mg, 1.07 mmol) was dissolved in 10 mL dry THF using sonication. This solution was added to a stirring solution of ligand **2** (50 mg, 0.134 mmol) dissolved in 1.07 mL dry THF. A fine yellow precipitate formed immediately upon addition. The yellow solid was collected on a fine frit and washed with copious THF to obtain 38 mg of product (0.076 mmol, 57% yield). IR n_{max} cm^{-1} (KBr pellet): 3486 (br), 3074 (w), 2062 (w), 1712 (s), 1598 (s), 1474 (m), 1435 (m), 1404 (m), 1384 (s), 1355 (m), 1255 (w), 1220 (s), 1161 (m), 1098 (m), 1063 (m), 1041 (w), 1014 (s), 982 (w), 947 (w), 837 (s), 799 (s), 729 (w), 694 (s), 668 (w), 660 (w), 639 (w), 621 (m). UV (1:1 ACN/water) λ_{max}, nm: 310, 316. ESI-MS (m/z): 462.0298.

4.3. Bioconjugation and purification

50 μL of a solution of cofactor **3** (1.99 mg/mL in 1:1 water/acetonitrile, 2.0 equiv) was added to a solution of protein scaffold (950 μL, 100 μM protein in Tris buffer, 25 mM pH 7.5 for Nb and 50mM pH 7.2 for tHisF) in a microcentrifuge tube and shaken in the dark at 4 °C for 1–2 h. The final concentrations were: 100 μM protein, 200 μM cofactor **3**, 2.5 vol% acetonitrile. Nb-C96-**3** was purified by four cycles of centrifugal filtration using 10 kDa cutoff spin filters (Millipore) with NaP_i buffer (100 mM, pH 7.0 with 10% ACN). The removal of excess cofactor was confirmed by HPLC analysis, and the conversion was estimated by ESI analysis.

4.4. General procedure for biocatalysis

A solution of Nb-C96-**3** (500 μL, 100 μM), 500 μL NaPi buffer (100 mM, pH 7.0 with 10% ACN), and 12.5 μL substrate (80 mM stock in ACN) were added to 1.5 mL microcentrifuge tube, and incubated at 4 °C for 15 min. 5 μL of peracetic acid aqueous solution (1M) was added to the mixture. The resulting solution shaken at 4 °C overnight. The final concentrations were: 1 mM substrate, 2.5 mM AcOOH, and 50 hybrid. The reaction was quenched by adding 350 μL DCM. pH was adjusted to 2 for ibuprofen case. The closed vials were agitated using a vortexer for 30s and centrifuged at 15000 rpm for 3 min. The organic layer was isolated. 10 μL sample was injected on HPLC.

Supplementary Material

Refer to Web version on PubMed Central for supplementary material.

Acknowledgments

This work was supported by The David and Lucile Packard Foundation and the NSF under the CCI Center for Selective C–H Functionalization (CHE-1205646). K.E.-G. is a trainee funded by an NIH Chemistry and Biology Interface Training Grant (T32 GM008720). MS data were acquired using instruments purchased using an NSF instrumentation grant (CHE-1048528). We thank Dr. Elena Solomaha at the UC Biophysics Core Facility for assistance with CD spectra.

References and notes

1. Davies HML, Morton D. Chem Soc Rev. 2011; 40:1857. [PubMed: 21359404]
2. Doyle MP, Duffy R, Ratnikov M, Zhou L. Chem Rev. 2010; 110:704. [PubMed: 19785457]
3. White MC. Science. 2012; 335:807. [PubMed: 22344434]
4. Kuhl N, Hopkinson MN, Wencel-Delord J, Glorius F. Angew Chem Int Ed. 2012; 51:10236.
5. Costas M, Chen K, Que L Jr. Coord Chem Rev. 2000; 200:517.
6. Talsi EP, Bryliakov KP. Coord Chem Rev. 2012; 256:1418.
7. Tanase, S.; Bouwman, E. Advances in Inorganic Chemistry. Vol. 58. Elsevier; 2006. Advances in Inorganic Chemistry; p. 29-75.
8. Davies HML, Manning JR. Nature. 2008; 451:417. [PubMed: 18216847]
9. Chen MS, White MC. Science. 2007; 318:783. [PubMed: 17975062]
10. Das S, Brudvig G, Crabtree R. J Am Chem Soc. 2008; 130:1628. [PubMed: 18197664]
11. Hull J, Sauer E, Incarvito C, Faller J, Brudvig G, Crabtree R. Inorg Chem. 2008; 48:488. [PubMed: 19093854]
12. Balcells D, Moles P, Blakemore JD, Raynaud C, Brudvig GW, Crabtree RH, Eisenstein O. Dalton Trans. 2009:5989. [PubMed: 19623399]

13. Das S, Incarvito CD, Crabtree RH, Brudvig GW. Science. 2006; 312:1941. [PubMed: 16809537]
14. Lewis JC. ACS Catal. 2013; 3:2954.
15. Kamijo S, Amaoka Y, Inoue M. Synthesis. 2010; 2010:2475.
16. Hull JF, Balcells D, Sauer ELO, Raynaud C, Brudvig GW, Crabtree RH, Eisenstein O. J Am Chem Soc. 2010; 132:7605. [PubMed: 20481432]
17. Steinreiber J, Ward TR. Top Organomet Chem. 2009; 25:93.
18. Oohora K, Kihira Y, Mizohata E, Inoue T, Hayashi T. J Am Chem Soc. 2013; 135:17282. [PubMed: 24191678]
19. Lewis JC, Arnold FH. CHIMIA. 2009; 63:309.
20. Fasan R. ACS Catal. 2012; 2:647.
21. Qi D, Tann C, Haring D, Distefano M. Chem Rev. 2001; 101:3081. [PubMed: 11710063]
22. Reetz MT, Rentzsch M, Pletsch A, Taglieber A, Hollmann F, Mondiere RJG, Dickmann N, Höcker B, Cerrone S, Haeger MC, Sterner R. Chem Bio Chem. 2008; 9:552.
23. Chen H, Tagore R, Das S, Incarvito C, Faller J, Crabtree R, Brudvig G. Inorg Chem. 2005; 44:7661. [PubMed: 16212393]
24. Maayan G, Yoo B, Kirshenbaum K. Tetrahedron Lett. 2008; 49:335. [PubMed: 19759852]
25. Constable EC, Ward MD. J Chem Soc Dalton Trans. 1990:1405.
26. Beismann-Driemeyer S, Sterner R. J Biol Chem. 2001; 276:20387. [PubMed: 11264293]
27. Bianchetti CM, Blouin GC, Bitto E, Olson JS, Phillips GN Jr. Proteins. 2009; 78:917. [PubMed: 19938152]
28. Yang H, Srivastava P, Zhang C, Lewis JC. Chem Bio Chem. 2013; 15:223.
29. Reetz MT, Rentzsch M, Pletsch A, Taglieber A, Hollmann F, Mondiere RJG, Dickmann N, Hoecker B, Cerrone S, Haeger MC, Sterner R. Chem Bio Chem. 2008; 9:552.
30. Onoda A, Fukumoto K, Arlt M, Bocola M, Schwaneberg U, Hayashi T. Chem Commun. 2012; 48:9756.
31. Hermanson, GT. Bioconjugate Techniques. Academic Press; San Diego, CA, 92101, USA: 1996.
32. Collot J, Humbert N, Skander M, Klein G, Ward TR. J Organomet Chem. 2004; 689:4868.
33. Reetz MT, Rentzsch M, Pletsch A, Maywald M, Maiwald P, Peyralans JJP, Maichele A, Fu Y, Jiao N, Hollmann F, Mondiere R, Taglieber A. Tetrahedron. 2007; 63:6404.
34. Creus M, Ward TR. Org Biomol Chem. 2007; 5:1835. [PubMed: 17551630]

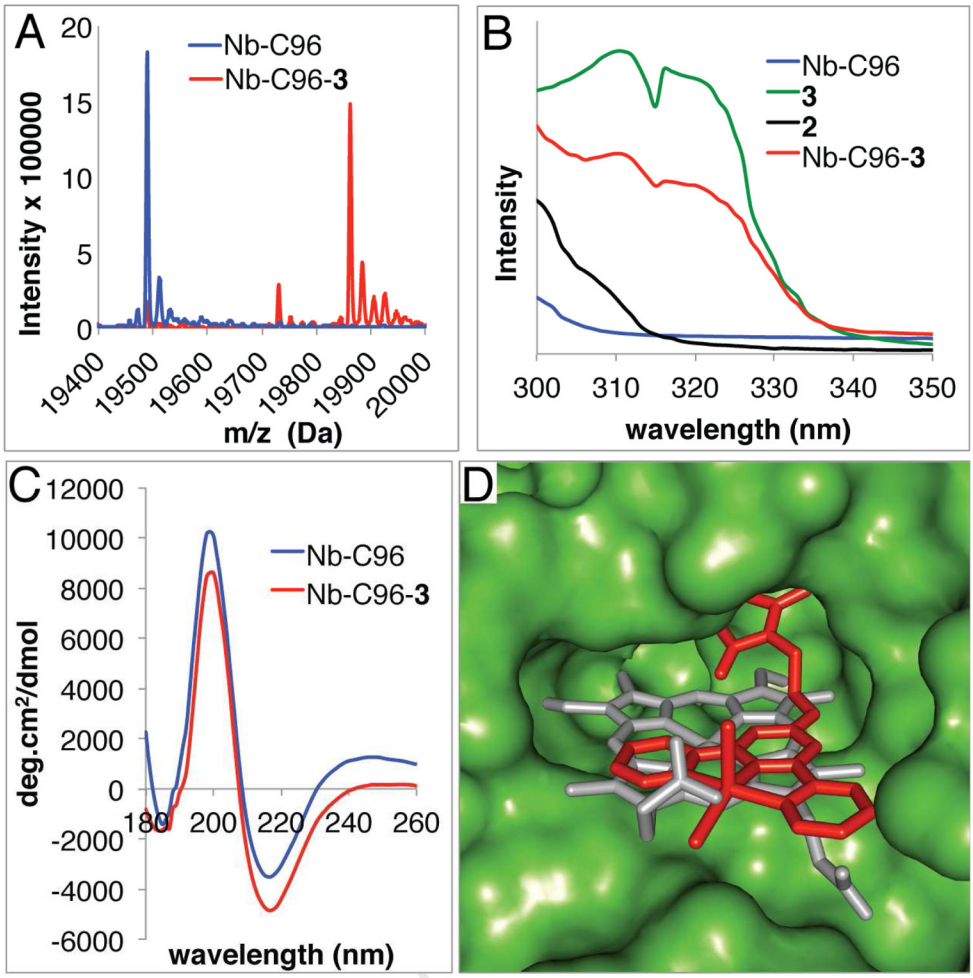

Figure 1.

A) HR ESI-MS spectra of Nb-C96 and Nb-C96-**3** showing the efficiency of Nb bioconjugation. B) UV spectra of Nb-C96, Nb-C96-**3**, **2**, and **3** showing the presence of $MnCl_2$ in Nb-C96-**3**. C) CD spectra of Nb-C96 and Nb-C96-**3** showing proper Nb folding following bioconjugation. D) Overlay of a DFT-optimized structure of **3** (red) covalently linked (Pymol) to a crystal structure of Nb (PDB ID 3EMM[27]) and the native heme (gray).

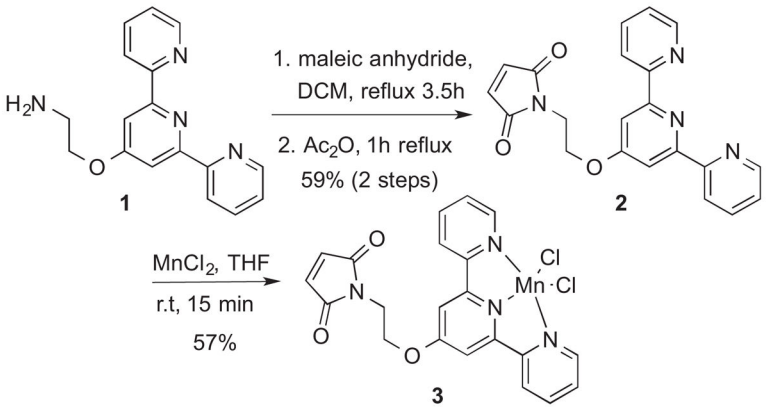

Scheme 1.
Synthesis of cofactor **3**

Table 1

Mass spectrometry and conversion data for ArMs

Entry	Scaffold (MW)[a]	Cofactor (MW)[b]	MW_{ArM}[a]	MW_{obs}[c]	Conv (%)[c]
1	tHisF-C48 (28754)	**3** (372)	29126	29128	40
2	tHisF-C48A50 (28712)	**3** (372)	29084	29082	85
3	Nb-C96 (19490)	**3** (372)	19862	19862	90
4	Nb-C125 (19547)	**3** (372)	19919	19919	95

[a] Protein MW calculated by using tools at http://www.scripps.edu/~cdputnam/protcalc.html.

[b] The $MnCl_2$ fragment not detected.

[c] Observed MW and approximate conversion from ESI-MS after 2h reaction.

Table 2

Optimization of ArM catalyzed oxidation[a]

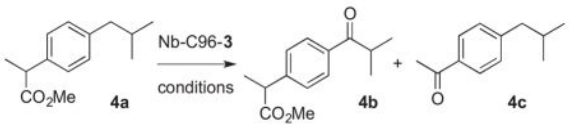

Entry	Solvent	Oxidant	Conv[b]. (%)
1	Tris (25mM, 7.0), 20%ACN	Oxone, 10eq	0
2	NaPi (100mM, 7.0), 20%ACN	Oxone, 10eq	77
3	NaPi (100mM, 7.0), 20%ACN	AcOOH, 10eq	85
4	NaPi (100mM, 7.0), 20%ACN	AcOOH, 2.5eq	83
5	NaPi (100mM, 7.0), 20%ACN	AcOOH, 2eq	76
6	NaPi (100mM, 7.0), 30%ACN	AcOOH, 2.5eq	12[e]
7	NaPi (100mM, 7.0), 10% ACN	AcOOH, 2.5eq	91
8	NaPi (100mM, 7.0)	AcOOH, 2.5eq	24
9[c]	NaPi (100mM, 7.0), 10% ACN	AcOOH, 2.5eq	45[e]
10[d]	NaPi (100mM, 7.0), 10% ACN	AcOOH, 2.5eq	58

[a] Reaction conditions: 1 mM substrate, 5% ArM, 4 °C, overnight in dark.

[b] Determined by GC analysis of DCM extract.

[c] Reaction conducted at room temperature

[d] 2.5% ArM loading used.

[e] Protein precipitation was observed.

Table 3

Substrate scope for ArM catalyzed oxidation

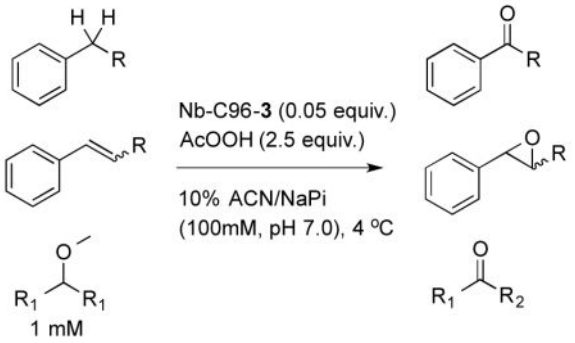

Entry	Substrate	Products (% conv.)	
1[a]	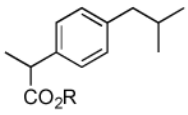	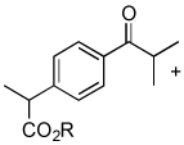	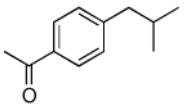
	4a (R=Me) **5a** (R=H)	**4b** (89) **5b** (87)	**4c** (7) **5c** (4)
2[b]	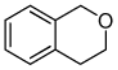	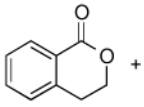	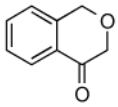
	6a	**6b** (82)	**6c** (15)
3[b]	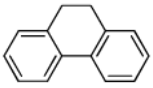	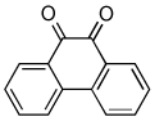	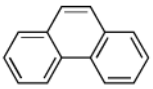
	7a	**7b** (17)	**7c** (11)
4[a]	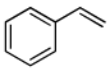	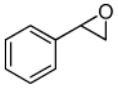	
	8a	**8b** (65)	
5[c]	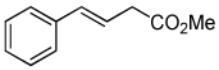	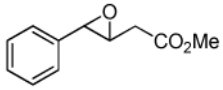	
	9a	**9b** (80)	
6[a]	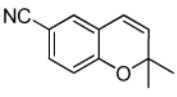	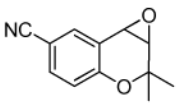	
	10a	**10b** (93)	

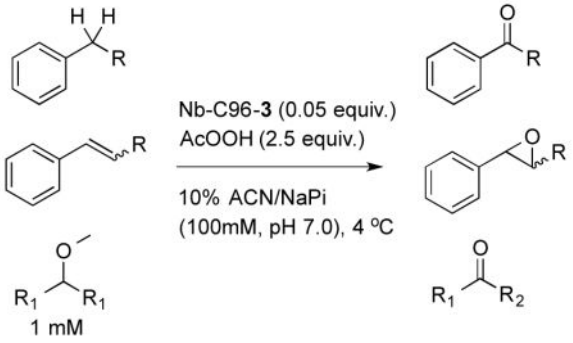

Entry	Substrate	Products (% conv.)
7[a]	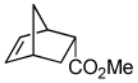	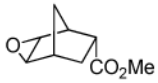
	11a	**11b** (99)
8[a]	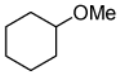	
	12a	**12b** (59)

[a] Conversion determined using GC integration values for starting materials and products.

[b] Conversion determined using ^{1}H-NMR signals for starting materials and products.

[c] Conversion determined using HPLC integration values for starting materials and products.